Inorganic Chemistry

Article

pubs.acs.org/IC

Dual-Functionalized Metal–Organic Frameworks Constructed from Hexatopic Ligand for Selective CO_2 Adsorption

Shi-Yuan Zhang, Xiaoping Zhang, Huimin Li, Zheng Niu, Wei Shi,* and Peng Cheng

Department of Chemistry, Key Laboratory of Advanced Energy Material Chemistry (MOE) and Collaborative Innovation Center of Chemical Science and Engineering (Tianjin),Nankai University, Tianjin 300071, P. R. China

Supporting Information

ABSTRACT: A ligand design approach, which requires rational design of ligand based on the knowledge of specific target, was applied for the synthesis of two interesting and robust MOFs **1** and **2** containing unusual several types of copper(II) secondary building units (SBUs). Thanks to unsaturated metal centers (UMCs) and azo group, microporous material **1** exhibited not only high CO_2 uptake but also an impressive selective adsorption of CO_2 over CH_4 and N_2. Moreover, a high H_2 uptake of **1** was also observed.

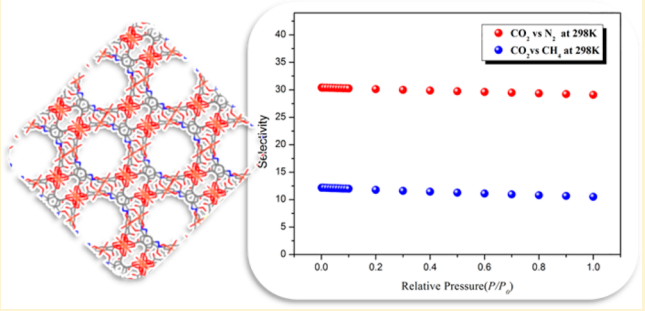

1. INTRODUCTION

Metal–organic frameworks (MOFs), constructed from metal-based nodes (metal ions or metal-oxo clusters) and linkers (multitopic organic ligands), have attracted tremendous interest.[1] Their modular nature with high surface area have made them a promising class of solid state porous materials for potential application in gas storage[2] and separation,[3] optical sensing[4] and catalysis.[5] More recently, great attention has been paid to energy/environment-related effluent CO_2 capture and separation using MOFs materials.[6] In addition to high gravimetric uptake and suitable thermodynamics and kinetics, the optimal MOFs for CO_2 separation should have ideal isosteric heat of adsorption (Q_{st}) that permits reversible physical adsorption–desorption process.[3b,7] Although numerous MOFs with diverse structural and topological types have been reported, rational design and assembly of functional crystalline solid represents a huge challenge to meet the specific criteria.

It is evident that crystal engineering[8] facilitates the development of targeted functional MOFs for CO_2 adsorption/separation. As exemplified by framework topology, secondary building units (SBUs)[9] and directional linkers together play a major role in the final CO_2 sorption behavior. One approach to improve CO_2 affinity and selectively of MOFs is to create unsaturated metal centers (UMCs) of SBUs.[10] Typically, UMCs are obtained by removing terminal ligands (e.g., H_2O, CH_3OH) upon heating under vacuum. The specific interaction exists between charge-dense binding sites of UMCs and CO_2, which attributes to the great quadrupole moment and polarizability of CO_2. The exploitation of $[Cu_2(CO_2)_4]$ paddlewheel SBU with axial open Cu^{2+} sites has achieved fruitful results since the earliest studies of HKUST-1, which has a relatively high Q_{st} of 29.2 kJ mol^{-1}.[11] Another strategy used to enhance CO_2 adsorption is the decoration of nitrogen-containing groups into MOFs. The N-containing groups serve as Lewis base sites with localized dipoles and induce the dispersion and electrostatic forces from the quadrupole moment of CO_2. The higher CO_2 uptake capacities at low pressure can be observed in amine modified MOFs compared with those of the parent materials.[12] Besides, other types of N-containing groups, for example, azo, triazole, tetrazole, acylamide, also offer an enhancement of CO_2-MOFs interactions, exhibiting high CO_2 uptake, Q_{st} and selectivity.[13]

With the aim to construct porous MOFs featuring aforementioned properties and based on our previous study,[14] we designed a hexacarboxylate ligand 1,2,3-tricarboxyl-(1′,2′,3′-tricarboxylazophenyl)benzene (H_6TTAB) processing polar and nonpolar regions, special orientations, and strong steric hindrance of carboxylate groups. High symmetrical polycarboxylate ligands, basically containing 1,3-benzenedicarboxylate moieties, will lead to a single SBU in crystal structure.[11a] In comparison, multiple types of SBUs can be generated with potential open Cu^{2+} sites by applying asymmetrical 1,2,3-tricarboxylate ligand.[15] Herein, we report the synthesis, crystal structures of two new MOFs $[Cu_6(TTAB)_2(\mu_2\text{-}OH_2)(H_2O)_8]\cdot(DMF)_4(H_2O)_6$ (**1**) and $H_2[Cu_6(TTAB)_2(\mu_3\text{-}OH)(\mu_2\text{-}OH)(H_2O)_8]\cdot(DMF)_{3.5}(H_2O)_6$ (**2**) that integrates unusual different types of SBUs. The gas adsorption behavior of **1** has also been investigated.

2. EXPERIMENTAL SECTION

2.1. Materials. The commercially available reagents were used without further purification.

2.1.1. Synthesis of H_6TTAB. The ligand H_6TTAB was synthesized according to the reported method.[16] Synthetic details are described as

Received: December 9, 2014
Published: February 19, 2015

DOI: 10.1021/ic502921j
Inorg. Chem. 2015, 54, 2310–2314

follow: A mixture of 5-nitrobenzene-1,2,3-tricarboxylic acid (2.55 g, 10 mmol), Zn (1.3 g, 20 mmol), and NaOH (1.2 g, 30 mmol) in a mixture of ethanol (50 mL) and water (20 mL) was heated under reflux. After 24 h, a yellow solid was obtained and collected by filtration. The resultant solid was dissolved in 50 mL of NaOH (aq, 1 M) and filtered to remove any insoluble solids. The filtrate was acidified to pH = 3 with HCl (aq, 3 M) to afford an orange precipitate. The yellow solid 1,2,3-tricarboxyl-(1′,2′,3′-tricarboxylazophenyl)-benzene (H_6TTAB) was obtained by filtration and dried in air (yield = 75%). ^{1}H NMR (400 MHz, $CDCl_3$): δ 8.39.

2.1.2. Synthesis of ***1****.* A mixture of $CuCl_2{\cdot}2H_2O$ (85 mg, 0.5 mmol), H_6TTAB (45 mg, 0.1 mmol), DMF (7.5 mL), and H_2O (7.5 mL) was sealed in a 23 mL Teflon-lined stainless steel vessel and heated at 90 °C for 3 days, and then cooled to room temperature. Dark green polyhedral crystals were obtained as a pure phase, washed by DMF, and dried at room temperature. Yield: 82%. IR (KBr, cm^{-1}): 3400s, 2930w, 2361m, 1643vs, 1423vs, 1367vs, 1257w, 1097m, 819m, 729m, 660m, 486m. Elemental analysis calcd (%) for **1**: C 31.60, H 3.65, N 6.14; found: C 31.54, H 3.76, N 6.48.

2.1.3. Synthesis of ***2****.* A mixture of $Cu(NO_3)_2{\cdot}6H_2O$ (122 mg, 0.5 mmol), H_6TTAB (45 mg, 0.1 mmol), DMF (5 mL), and H_2O (10 mL) was sealed in a 23 mL Teflon-lined stainless steel vessel and heated at 100 °C for 3 days, and then cooled to room temperature. Yellow green rod-like crystals were obtained as a pure phase, washed by DMF, and dried at room temperature. Yield: 76%. IR (KBr, cm^{-1}): 3424vs, 2964vs, 2916m, 2853w, 2361m, 1618s, 1578s, 1456s, 1419s, 1383vs, 1045m, 800w, 723m, 662w. Elemental analysis calcd (%) for **2**: C 30.62, H 3.68, N 5.76; found: C 30.39, H 3.31, N 6.06.

2.2. Physical Measurements. Elemental analysis was performed on a Perkin−Elmer 240 CHN elemental analyzer. ^{1}H NMR spectrum was recorded with a Bruker AV 400 spectrometer at 400 MHz. Chemical shifts (δ values) were reported in ppm from internal Me_4Si. IR spectra were recorded in the range 400−4000 cm^{-1} on a Bruker TENOR 27 spectrophotometer by using KBr pellets. Powder X-ray diffraction measurements were recorded on a Rigaku D/Max-2500 X-ray diffractometer using Cu Kα radiation. Thermal analyses (N_2 atmosphere, heating rate of 1.5 °C/min) were carried out in a Labsys NETZSCH TG 209 Setaram apparatus.

2.2.1. X-ray Structure Determination. The crystallographic data were collected by an Oxford Supernova Single Crystal Diffractometer equipped with graphite monochromatic Mo Kα radiation (λ = 0.71073 Å). Structures were solved by direct methods with SHELXS program and refined by full-matrix least-squares techniques against F^2 with the SHELXL program package.[17] All non-hydrogen atoms were refined anisotropically except O14 in **1**, and hydrogen atoms were located and refined isotropically. The contribution of disordered solvent molecules was treated as a diffuse using the Squeeze procedure in PLATON.[18] The resulting new HKL4 files were used to further refine the structures. Crystallographic data are shown in Table 1. CCDC-1029791 and -1029792 (**1** and **2**) contain the supplementary crystallographic data for this paper. These data can be obtained free of charge via www.ccdc.cam.ac.uk.

2.2.2. Low-Pressure Sorption Experiments. All gas-adsorption experiments were performed on a Quantachrome IQ_2 automatic volumetric instrument. All gases used were of 99.999% purity. The methanol solvent-exchanged sample was degassed at 100 °C for 12h to remove the guest molecules. The temperature for N_2, H_2, and Ar sorption experiments was controlled by a refrigerated bath of liquid nitrogen (77 K) or liquid argon (87 K). The N_2 and Ar sorption isotherms were recorded over the pressure range 10^{-7}−1 bar at 77 and 87 K, respectively. The H_2 sorption isotherms (77 and 87 K) were carried out over the pressure range 10^{-3}−1 bar. The CO_2, CH_4, and N_2 sorption isotherms (273 and 298 K) were measured in a temperature-controlled water bath over the pressure range 10^{-3}−1 bar.

3. RESULTS AND DISCUSSION

3.1. Synthesis and Structures of 1 and 2. Dark green crystals of **1** are obtained under solvothermal reaction of $CuCl_2{\cdot}2H_2O$ with H_6TTAB in *N*,*N*-dimethylformamide (DMF) and water at 90 °C for 3 days. Single-crystal X-ray diffraction analysis reveals that it crystallizes in orthorhombic space group *Pnma*. The framework is built from two types of dimer SBUs joined by 6-connected TTAB linker (Figure 1). One type of dimer is paddlewheel SBU composed from two Cu^{2+} and four carboxylate groups; the other one contains two square pyramids Cu^{2+} that share one central μ_2-oxo anion. Both

Table 1. Crystal Data and Structure Refinement Details of 1 and 2

	1	2
formula	$C_{48}H_{66}N_8Cu_6O_{43}$	$C_{46.5}H_{66.5}N_{7.5}Cu_6O_{44.5}$
fw	1824.34	1823.83
temp (K)	150(2)	150(2)
cryst system	orthorhombic	monoclinic
space group	*Pnma*	*C*2/*c*
a (Å)	19.348(2)	29.303(3)
b (Å)	21.110(2)	16.853(1)
c (Å)	19.822(2)	26.713(2)
β (deg)	90.00	105.027(8)
V (Å^3)	8096.2(14)	12740.8(17)
Z	4	8
Dc (g·cm^{-3})	1.497	1.901
μ (mm^{-1})	1.642	2.083
F (000)	2824	5744
R_{int}	0.0455	0.0381
GOF	1.039	0.917
R_1 (I > 2σ(I))	0.0528	0.0681
R_2 (all data)	0.1231	0.1780
$\Delta\rho_{max}$ (e Å^{-3})	1.48	1.97
$\Delta\rho_{min}$ (eÅ^{-3})	−0.66	−1.76

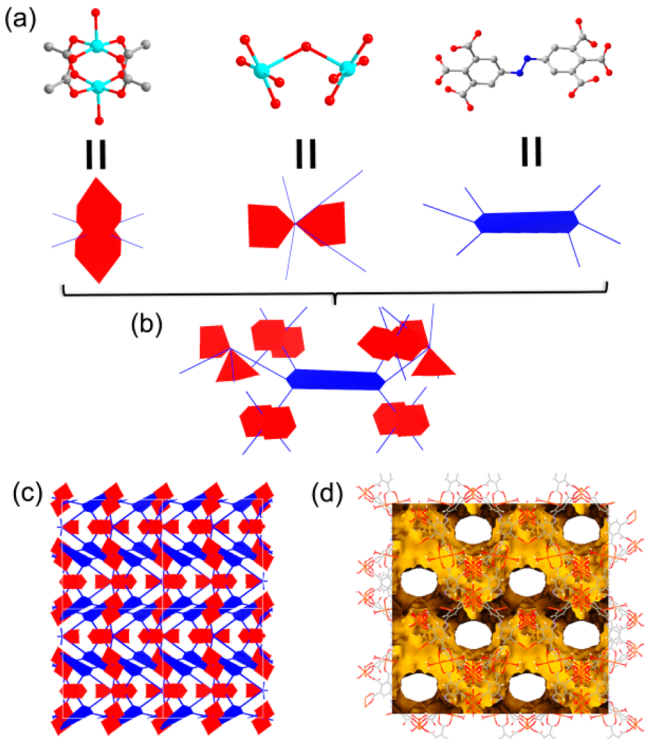

Figure 1. (a) Schematic representation of copper SBUs and hexacarboxylate TTAB^{6-} ligand. (b) Linkage of 4-connected copper SBUs and 6-connected TTAB^{6-}. (c) Schematic view of 3D framework of **1**. (d) 1D channels within 3D framework of **1**.

DOI: 10.1021/ic502921j
Inorg. Chem. 2015, 54, 2310−2314

dimer units are linked by four separate hexatopic organic linkers to build up the 3D structure. The removal of terminal coordinated water molecules of both dimers can generate UMCs with open Cu^{2+} sites. Topology analysis reveals that **1** adopts a 4,4,4,6-c 4-nodal network with Schlafli symbol of $\{4^2.6^2.8^2\}\{4^4.6^2\}_2\{4^5.6^8.8^2\}_2$ (Supporting Information Figure S1). Careful examination of **1** shows that it has 1D solvent accessible channel along [100] direction with an effective diameter estimated to be 10.3 Å (considering van der Waals radii). It is noteworthy that the dumbbell-shaped channels and zigzag channels are also found along [010] and [001] directions (Supporting Information Figure S2). The total free volume of **1** with removal of guest molecules is 53.4% (4320.0 $Å^3$ of the unit cell volume of 8096.2 $Å^3$) by PLATON.[18]

Solvothermal reaction of $Cu(NO_3)_2{\cdot}6H_2O$ with H_6TTAB in DMF and water at 100 °C for 3 days yields yellow green rod-like crystals of **2**. The crystallographic analysis reveals that **2** crystallizes in monoclinic space group C/2c and adopts an unprecedented 3,4,5,6,8-connected network topology. As shown in Figure 2, the structure of **2** contains two

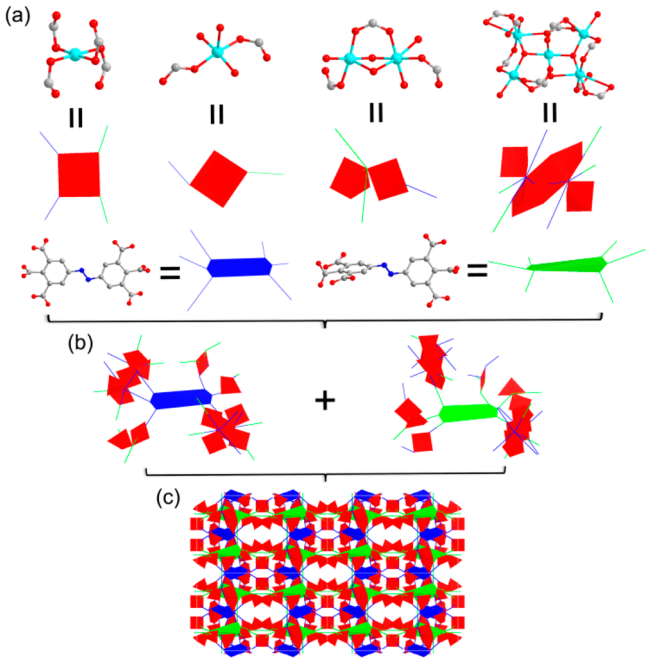

Figure 2. (a) Schematic representation of four types of copper SBUs and hexacarboxylate $TTAB^{6-}$ ligand. (b) Linkage of copper SBUs and $TTAB^{6-}$. (c) Schematic view of 3D framework of **2**.

crystallographically independent $TTAB^{6-}$ ligands and four types of Cu^{2+} SBUs. Four monodentated carboxylate groups from four different $TTAB^{6-}$ ligands coordinate to Cu^{2+} center that forms 4-connected (4-c) SBU. The 2-c SBU is based on a five coordinated Cu^{2+} ion. The 3-c dimer SBU contains an octahedral and a square pyramid sharing two μ_2-oxo anions. The 8-c penta-copper SBU can be regarded as the junction of two Cu_3O clusters. Specifically, the center Cu^{2+} adopts octahedral coordination geometry, while the other two are five coordinated. The μ_3-O lies in the C_3 axis of three Cu^{2+} atoms. It should be noted that water molecules in 2-c, 3-c and 8-c SBUs would generate potential UMCs through desolvation. The $TTAB^{6-}$ ligands serve as 6-c nodes that further link these Cu^{2+} SBUs. As a consequence, the assembly of these different types of nodes results in a rare 3,4,5,6,8-c 5-nodal network (Supporting Information Figure S3). The topological point symbol of **2** is $\{4{\cdot}5{\cdot}6\}_2\{4^2{\cdot}5^2{\cdot}6{\cdot}7\}\{4^4{\cdot}5^4{\cdot}6^2\}_2\{4^4{\cdot}5^4{\cdot}6^4{\cdot}7^2{\cdot}8\}_2\{4^6{\cdot}5^{14}{\cdot}7^6{\cdot}8^2\}$.

The control over structural features of **1** and **2** attributes to the flexibility of $TTAB^{6-}$ ligand, temperature and DMF/H_2O ratio. In **1**, two phenyl groups of $TTAB^{6-}$ are nearly perpendicular to each other with an angle of 80.54°; while the angles in **2** are reduced to 56.45° and 10.49°. Increased temperature can provide higher energy thus facilitates the rotation between two phenyl groups. In fact, the orientation of $TTAB^{6-}$ ligand is responsible for the alignment of SBUs, resulting in the structural variation of **1** and **2**. In the other aspect, the increased water amount during synthesis facilitates the formation of different types of SBUs with terminal water molecules, as evidenced by the DMF/H_2O ratio in the formulas. Indeed, more types of SBUs require certain arrangement of $TTAB^{6-}$ ligands by rotation, which in turn lower the symmetry of the lattice.

The phase purity of the bulk crystalline materials of **1** and **2** was confirmed by similarities between the calculated and as-synthesized powder X-ray diffraction (PXRD) patterns, respectively (Supporting Information Figure S4). The thermogravimetric curve of **1** indicates an initial weight loss of 31.0% from 25 to 110 °C, corresponding to the loss of coordinated water molecules and guest molecules (calcd 31.5%). While **2** exhibits a gradual weight loss of 5.5% from 25 to 200 °C (Supporting Information Figure S5), corresponding to the loss of guest water molecules (calcd 5.9%). At 237.5 °C, a weight loss of 29.1% is observed, indicating the loss of DMF and coordinated water molecules (calcd 28.1%).

3.2. Gas Absorption Properties of 1. The interesting structural and functional features of **1**, that is, the narrow channels with UMCs and localized dipoles of azo groups, prompted us to evaluate the gas sorption behavior. Powder XRD of MeOH-exchanged sample and activated sample indicate the stability of the framework (Supporting Information Figure S6). The permanent porosity has been confirmed by individual N_2 and Ar adsorption isotherm at 77 and 87 K (Supporting Information Figure S7). **1** exhibits a type I isotherm characteristic of microporous materials and reveals an overall uptake of 347 (N_2) and 388 (Ar) $cm^3\ g^{-1}$ at 1 bar. The apparent surface corresponds to a Brunauer–Emmet–Teller (BET) surface area of 1224 (N_2) and 1382 (Ar) $cm^3\ g^{-1}$ and a Langmuir surface area of 1393 (N_2) and 1573 (Ar) $cm^3\ g^{-1}$, respectively. The volumetric H_2 uptakes in **1** were collected at 77 and 87 K (Supporting Information Figure S8). All H_2 isotherms exhibit rapid kinetics and good reversibility with H_2 uptake capacity of 186.1 $cm^3\ g^{-1}$ (1.66 wt %) at 77 K and 1.0 bar, and 131.5 $cm^3\ g^{-1}$ (1.17 wt %) at 87 K and 1.0 bar. Moreover, Q_{st} for H_2 was determined by Clausius–Clapeyron equation and estimated to be 8.34 kJ mol^{-1} at zero coverage (Supporting Information Figure S9). These values in H_2 capacity and Q_{st} are comparably higher than those of previously reported porous MOFs.[2b]

The special dual-functionalities in **1** prompt us to further explore the potential applications toward CO_2 capture and separation. We have measured low pressure CO_2, CH_4 and N_2 sorption data at 273 and 298 K, as shown in Figure 3. The CO_2 uptake capacity of **1** reaches 140.0 $cm^3\ g^{-1}$ at 273 K and 81.2 $cm^3\ g^{-1}$ at 298 K, respectively, which is relatively high compared to other classes of porous materials.[3] Without the large surface area and free volume, we attribute the high CO_2 uptake to UMCs and azo groups, which serve as potential

DOI: 10.1021/ic502921j
Inorg. Chem. 2015, 54, 2310–2314

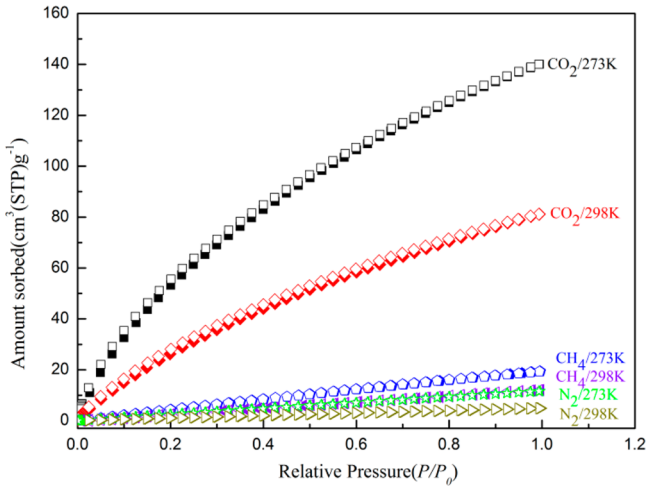

Figure 3. Sorption isotherms for CO_2, CH_4, and N_2 at 273 and 298 K. (Adsorption and desorption branches are shown with closed and open symbols, respectively.)

binding sites for CO_2 that facilitate the dipole−quadrupole interactions. The Q_{st} for CO_2 was calculated to be 27.4 kJ mol^{-1} by fitting the 273 and 298 K isotherms to the virial equation, indicating high affinity toward CO_2 at low loading (Supporting Information Figure S10 and Table S1). For comparison, the CH_4 and N_2 uptakes for **1** at 1 atm were found to be 19.3 and 11.6 cm^3 g^{-1} at 273 K, 10.4 and 4.8 cm^3 g^{-1} at 298 K, respectively. To predict the CO_2 separation performance of **1** at 298 K, ideal adsorbed solution theory (IAST)[19] calculations were used for binary gas adsorption selectivity under practically relevant conditions (Figure 4). In particular, **1** shows a high

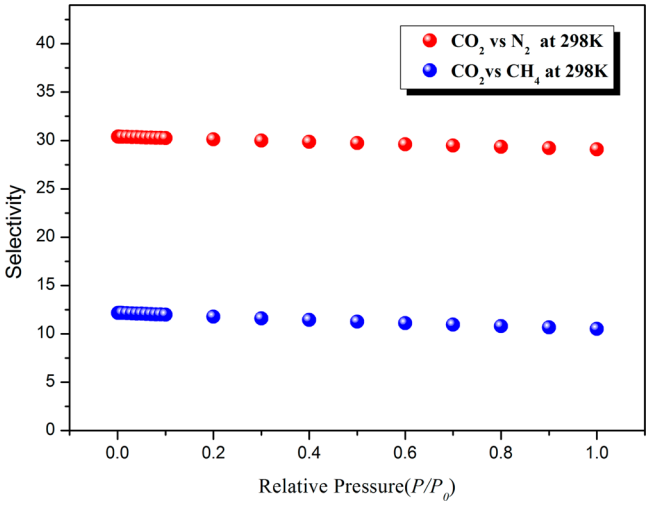

Figure 4. Calculated selectivity of CO_2/CH_4 (50:50) and CO_2/N_2 (10:90) at 298 K, respectively.

CO_2/N_2 selectivity of 29.1 in a 10:90 molar ratio of CO_2 and N_2 mixture at 1 bar. The calculated CO_2/CH_4 selectivity is 10.5 at 1 bar from equimolar CO_2 and CH_4 mixture. The selectivity of **1** for CO_2 over CH_4 and N_2 under these conditions is comparable to the majority of MOFs reported to date.[3a,6b] Indeed, many MOFs with high selectivity have lower CO_2 uptake than **1**.[3] Therefore, this material would be a promising candidate for natural gas purification and postcombustion CO_2 capture applications.

4. CONCLUSIONS

In conclusion, a hexacarboxylate ligand containing azo group has been successfully used for the construction of MOFs, **1** and **2**, showing dual-functionalities and novel topologies. Microporous MOF **1** exhibits a hydrogen uptake capacity of 1.66 wt % at 77 K and 1 bar and a high CO_2 uptake of 140.0 cm^3 g^{-1} at 273 K. The utilization of UMCs and N-containing moieties affords enhanced Q_{st} and uptakes because of their special interactions with gas molecules. The high CO_2 affinity over CH_4 and N_2, particularly at low pressure certainly renders **1** a prospective material for low CO_2 concentration purification. These highly desirable features in the context of the multicomponent gas adsorption will be needed to develop MOFs for industrial applications.

■ ASSOCIATED CONTENT

Ⓢ Supporting Information

Additional single crystal X-ray analysis figures, powder X-ray diffraction data, thermogravimetic measurements, gas sorption data, and analyzing details. This material is available free of charge via the Internet at http://pubs.acs.org.

■ AUTHOR INFORMATION

Corresponding Author

*E-mail: shiwei@nankai.edu.cn.

Notes

The authors declare no competing financial interest.

■ ACKNOWLEDGMENTS

We thank the "973 program" (2012CB821702), the MOE (NCET-13-0305, IRT-13R30 and IRT13022), and 111 Project (B12015) for financial support.

■ REFERENCES

(1) (a) Moulton, B.; Zaworotko, M. J. *Chem. Rev.* **2001**, *101*, 1629−1658. (b) Kitagawa, S.; Kitaura, R.; Noro, S.-i. *Angew. Chem., Int. Ed.* **2004**, *43*, 2334−2375. (c) Batten, S. R.; Neville, S. M.; Turner, D. R. *Coordination Polymers: Design, Analysis and Application*; Royal Society of Chemistry: Cambridge, U.K., 2009. (d) *Metal−Organic Frameworks: Design and Application*; MacGillivray, L. R., Ed.; Wiley & Sons, Inc.: Hoboken, NJ, 2010.

(2) (a) Li, J.-R.; Ma, Y.; McCarthy, M. C.; Sculley, J.; Yu, J.; Jeong, H.-K.; Balbuena, P. B.; Zhou, H.-C. *Coord. Chem. Rev.* **2011**, *255*, 1791−1823. (b) Suh, M. P.; Park, H. J.; Prasad, T. K.; Lim, D. W. *Chem. Rev.* **2012**, *112*, 782−835. (c) He, Y.; Zhou, W.; Qian, G.; Chen, B. *Chem. Soc. Rev.* **2014**, *43*, 5657−5678.

(3) (a) Li, J.-R.; Sculley, J.; Zhou, H.-C. *Chem. Rev.* **2012**, *112*, 869−932. (b) Sumida, K.; Rogow, D. L.; Mason, J. A.; McDonald, T. M.; Bloch, E. D.; Herm, Z. R.; Bae, T.-H.; Long, J. R. *Chem. Rev.* **2012**, *112*, 724−781.

(4) (a) Kreno, L. E.; Leong, K.; Farha, O. K.; Allendorf, M.; Van Duyne, R. P.; Hupp, J. T. *Chem. Rev.* **2012**, *112*, 1105−1125. (b) Cui, Y.; Chen, B.; Qian, G. *Coord. Chem. Rev.* **2014**, *273*, 76−86.

(5) Lee, J.; Farha, O. K.; Roberts, J.; Scheidt, K. A.; Nguyen, S. T.; Hupp, J. T. *Chem. Soc. Rev.* **2009**, *38*, 1450−1459.

(6) (a) Nugent, P.; Belmabkhout, Y.; Burd, S. D.; Cairns, A. J.; Luebke, R.; Forrest, K.; Pham, T.; Ma, S.; Space, B.; Wojtas, L.; Eddaoudi, M.; Zaworotko, M. J. *Nature* **2013**, *495*, 80−84. (b) Zhang, Z.; Zhao, Y.; Gong, Q.; Li, Z.; Li, J. *Chem. Commun.* **2013**, *49*, 653−661.

(7) Sayari, A.; Belmabkhout, Y.; Serna-Guerrero, R. *Chem. Eng. J.* **2011**, *171*, 760−774.

(8) Desiraju, G. R. *Angew. Chem., Int. Ed.* **2007**, *46*, 8342−8356.

DOI: 10.1021/ic502921j
Inorg. Chem. 2015, 54, 2310−2314

(9) (a) Rosi, N. L.; Kim, J.; Eddaoudi, M.; Chen, B.; O'Keeffe, M.; Yaghi, O. M. *J. Am. Chem. Soc.* **2005**, *127*, 1504−1518. (b) Perry, J. J.; Perman, J. A.; Zaworotko, M. J. *Chem. Soc. Rev.* **2009**, *38*, 1400−1417.
(10) (a) Chen, B.; Xiang, S.; Qian, G. *Acc. Chem. Res.* **2010**, *43*, 1115−1124. (b) Caskey, S. R.; Wong-Foy, A. G.; Matzger, A. J. *J. Am. Chem. Soc.* **2008**, *130*, 10870−10871.
(11) (a) Chui, S. S.-Y.; Lo, S. M.-F.; Charmant, J. P. H.; Orpen, A. G.; Williams, I. D. *Science* **1999**, *283*, 1148−1150. (b) Montoro, C.; Garcia, E.; Calero, S.; Perez-Fernandez, M. A.; Lopez, A. L.; Barea, E.; Navarro, J. A. R. *J. Mater. Chem.* **2012**, *22*, 10155−10158. (c) Bordiga, S.; Regli, L.; Bonino, F.; Groppo, E.; Lamberti, C.; Xiao, B.; Wheatley, P. S.; Morris, R. E.; Zecchina, A. *Phys. Chem. Chem. Phys.* **2007**, *9*, 2676−2685.
(12) (a) Millward, A. R.; Yaghi, O. M. *J. Am. Chem. Soc.* **2005**, *127*, 17998−17999. (b) Couck, S.; Denayer, J. F. M.; Baron, G. V.; Remy, T.; Gascon, J.; Kapteijn, F. *J. Am. Chem. Soc.* **2009**, *131*, 6326−6327. (c) Vaidhyanathan, R.; Iremonger, S. S.; Shimizu, G. K. H.; Boyd, P. G.; Alavi, S.; Woo, T. K. *Science* **2010**, *330*, 650−653. (d) Li, B.; Zhang, Z.; Li, Y.; Yao, K.; Zhu, Y.; Deng, Z.; Yang, F.; Zhou, X.; Li, G.; Wu, H.; Nijem, N.; Chabal, Y. J.; Lai, Z.; Han, Y.; Shi, Z.; Feng, S.; Li, J. *Angew. Chem., Int. Ed.* **2012**, *51*, 1412−1415.
(13) (a) Zeleňák, V.; Vargová, Z.; Almáši, M.; Zeleňáková, A.; Kuchár, J. *Microporous Mesoporous Mater.* **2010**, *129*, 354−359. (b) Lin, J.-B.; Xue, W.; Zhang, J.-P.; Chen, X.-M. *Chem. Commun.* **2011**, *47*, 926−928. (c) Li, J.-R.; Tao, Y.; Yu, Q.; Bu, X.-H.; Sakamoto, H.; Kitagawa, S. *Chem.−Eur. J.* **2008**, *14*, 2771−2776. (d) Zheng, B.; Bai, J.; Duan, J.; Wojtas, L.; Zaworotko, M. J. *J. Am. Chem. Soc.* **2010**, *133*, 748−751.
(14) (a) Li, H.; Shi, W.; Zhao, K.; Niu, Z.; Li, H.; Cheng, P. *Chem.−Eur. J.* **2013**, *19*, 3358−3365. (b) Li, H.; Shi, W.; Zhao, K.; Niu, Z.; Chen, X.; Cheng, P. *Chem.−Eur. J.* **2012**, *18*, 5715−5723.
(15) Gutschke, S. O. H.; Price, D. J.; Powell, A. K.; Wood, P. T. *Angew. Chem., Int. Ed.* **2001**, *40*, 1920−1923.
(16) Wang, S.; Wang, X.; Li, L.; Advincula, R. C. *J. Org. Chem.* **2004**, *69*, 9073−9084.
(17) Sheldrick, G. *Acta Crystallogr.* **2008**, *A64*, 112−122.
(18) Spek, A. L. *J. Appl. Crystallogr.* **2003**, *36*, 7−13.
(19) Myers, A. L.; Prausnitz, J. M. *AIChE J.* **1965**, *11*, 121−127.

DOI: 10.1021/ic502921j
Inorg. Chem. 2015, 54, 2310−2314